frontiers | Frontiers in Mechanical Engineering

TYPE Original Research
PUBLISHED 14 March 2025
DOI 10.3389/fmech.2025.1397832



OPEN ACCESS

EDITED BY
Xuping Zhang,
Aarhus University, Denmark

REVIEWED BY
Bin Yang,
Xi'an Jiaotong University, China
Yanfeng Peng,
Hunan University of Science and Engineering, China

*CORRESPONDENCE
Ziqiang Qiao,
zqqiao90@163.com

RECEIVED 08 March 2024
ACCEPTED 24 February 2025
PUBLISHED 14 March 2025

CITATION
Liu J and Qiao Z (2025) Kinematic analysis of wire stripping for distribution robots based on wire stripping and cutting force control algorithm under cylindrical gear transmission. *Front. Mech. Eng.* 11:1397832.
doi: 10.3389/fmech.2025.1397832



# Kinematic analysis of wire stripping for distribution robots based on wire stripping and cutting force control algorithm under cylindrical gear transmission

Juan Liu and Ziqiang Qiao*

School of Mechanical and Electrical Engineering, Huanghe JiaoTong University, Jiaozuo, China

**Introduction:** The accurate analysis of Wire Stripping Operation of Power Distribution Robot is crucial for the automation and intelligence of power system maintenance operations. Therefore, a new design and control method for Wire Stripping Operation of Power Distribution Robot has been proposed.

**Methods:** Firstly, a wire stripping device suitable for Cylindrical Gear Transmission was designed. Then, kinematic analysis was conducted based on the Wire Stripping and Cutting Force to ensure the accuracy of the stripping process. Finally, to cope with changes in stiffness environments, an impedance control strategy based on Recursive Least Square method was introduced to improve the stability and adaptability of the control system.

**Results:** These results confirmed that the proposed method performs significantly better than traditional methods in force response tracking. When the wire stripping time was 1.9 s, the sinusoidal force responses of the research method, reference force, and general impedance force were −15.3 N, −15.4 N, and −8.2 N, respectively. The sinusoidal force tracking responses were −19.6 N, 6.5 N, 2.6 N to −18.2 N, respectively. The impedance force error curve of the proposed method shows no significant difference compared to the general impedance force error curve ($P < 0.05$). Meanwhile, the impedance force error curve of the research method was more stable, while the general impedance force error curve fluctuated greatly. Simulation analysis confirmed that the wire stripping surface of the research method was smooth and undamaged, demonstrating the rationality of the wire stripping device design and the superiority of the wire stripping control algorithm. The accuracy, efficiency, and stability scores of the proposed method are superior to the other three classical control methods.

**Discussion:** This study is crucial for improving the automation level and operational accuracy of wire stripping operations in power distribution robots.

KEYWORDS

**cylindrical gear transmission, wire stripping and cutting force, control algorithm, power distribution robot, wire stripping motion, RLS**

# 1 Introduction

Due to the continuous improvement of automation in the power industry, Power Distribution Robot (PDR) has played an increasingly important role in the maintenance and operation of the power system. Performing a Wire Stripping Operation (WSO) on cables is a fundamental and crucial step in ensuring stable operation of the power system. It requires precise removal of the outer protective layer of the cable to expose the inner conductor without damaging the conductor itself (Arastou et al., 2022). Traditional manual WSO often leads to low efficiency and potential security risks due to uncontrollable operational forces and environmental factors. In view of this, how to improve the accuracy of WSO and ensure safe and efficient completion of tasks has become a hot research topic. Cylindrical Gear Transmission (CGT) has been widely used in mechanical transmission due to its compact structure, high transmission efficiency, and strong adaptability. By utilizing the characteristics of CGT, PDR can execute WSO in a more precise and stable manner (Roberts and Florentine, 2021). However, the complexity of WSO requires robots to have a high motion control capability, which involves precise management of Wire Stripping and Cutting Force (WSCF) and in-depth analysis of robot kinematics. The WSCF control algorithm is a control technology specifically designed for WSO, which can dynamically adjust the cutting force based on specific parameters such as material and thickness, thereby avoiding damage to the conductor (Amin et al., 2020). This type of algorithm combines the advantages of CGT to achieve high-precision control of PDR wire stripping actions. The innovation of this study lies in the combination of WSCF control algorithm and Recursive Least Square (RLS) to better achieve PDR wire stripping motion. This study will delve into the wire stripping kinematics of PDR under CGT, with the goal of achieving high-precision and high stability WSO under different operating conditions through the combination of kinematic analysis and related control technologies. This study mainly consists of four parts. Firstly, there is a literature review that summarizes the research results on different robots and controls. Secondly, there is research methodology, including the design of PDR wire stripping and kinematic analysis of PDR wire stripping based on WSCF control algorithm. Then comes the result analysis, mainly conducting simulation analysis on the research methods. Finally, the conclusion summarizes the research findings and shortcomings.

# 2 Literature review

With the advancement of technology and the growth of social demand, there have been many studies on robot cable stripping technology. Zhang et al. proposed a control method for a peeling robot based on kinematic analysis and error compensation. The experimental results show that the positioning accuracy of the robot in cable stripping is significantly improved, and the cutting error is reduced by 30%. However, research has not fully considered the impact of changes in meshing stiffness in gear transmission on stripping accuracy, and there may be significant errors in practical applications (Zhang et al., 2023). Bieze et al. proposed a real-time control method for peeling based on dual sensors, which maintains the stability of peeling quality under different tension conditions, with tension error controlled within 5%. But the system structure is complex and the maintenance cost is high (Bieze et al., 2020). Zhao et al. and other experts have proposed a real-time monitoring method for wire stripping force based on machine vision technology to meet the high precision requirements of the power industry for operation robots. This method controls the wire stripping error within 1 mm in practical applications and improves the wire stripping efficiency by 20%. But in complex environments, it may be affected by external factors such as lighting, which can affect recognition performance (Zhao et al., 2023). Xu et al. and other experts proposed an automated peeling system based on dual arm robots, which controls the cutting action through a distributed control system to ensure synchronous cable peeling and cutting. The results show that the dual arm robot can efficiently complete cutting tasks, with a 40% increase in efficiency compared to traditional methods (Xu et al., 2022). Brahmi *et al.* have proposed a feedback control based cable cutting robot to address the issue of inconsistent cable materials and thicknesses. The robot adjusts its cutting tasks in real-time using fuzzy algorithms to ensure the quality of cable stripping. The results indicate that this method has high accuracy in cutting cables made of high hardness materials. However, the system response is slow during the cutting process, and there is room for improvement in efficiency (Brahmi et al., 2020).

With the development of technology, especially in electronics, computing, and information technology, the demand for more complex and advanced control systems is constantly increasing. These systems aim to improve the performance and efficiency of various applications, including manufacturing, transportation, energy systems, biomedical engineering, and robotics. Li et al. proposed a causal control strategy based on optimized approximate transfer functions to address non-causal issues in wave energy control. These experiments confirmed that this strategy enabled the lift sink absorber to effectively extract wave energy up to 90% of the theoretical upper limit. Meanwhile, this controller had a certain sensitivity to the viscous damping effect caused by resistance and spectral bandwidth. However, its sensitivity to viscous damping effects also exposes certain limitations. Further research is needed to maintain the robustness of control systems under uncertain external conditions (Li and Gao, 2020). Jiang et al. proposed a hierarchical control strategy based on model free adaptive sliding mode control for path tracking and energy-saving control of six wheel independent drive unmanned ground vehicles. The upper and lower controllers adopted different methods to achieve effective combination of lateral torque and longitudinal force. These experiments confirmed that the control strategy exhibited good control performance and optimized energy-saving characteristics, which could ensure the vehicle stability. However, further research is needed on how to combine different levels of control strategies to achieve optimal system performance (Jiang et al., 2022). Stefenon et al. proposed a potential distribution evaluation method based on finite element method to address the reliability and potential optimization issues of intermediate obstacles in compact distribution networks. By analyzing the surface potential distribution on insulators, this method effectively improves the design and performance of

distribution network components, but there is still room for optimization in the control accuracy and reliability of the system (Stefenon et al., 2022).

Through the above research, optimizing the control of robots can improve their related performance, but most of them focus on single application scenarios or specific task control. And there is no attention paid to the comprehensive control requirements of robot systems in multi task and multi scenario scenarios, especially the robustness and energy efficiency optimization of control strategies in complex dynamic environments. Therefore, in order to improve the motion control performance of PDR wire stripping action, this study conducted a detailed kinematic analysis of the wire stripping kinematics of PDR under CGT, aiming to further improve its operational efficiency and accuracy, and ensure the reliability and safety of power system maintenance operations. The research innovation lies in the design of a cable stripping device suitable for cylindrical gear transmission, combined with kinematic analysis based on cutting force control algorithm. Secondly, the study adopted an impedance control strategy based on recursive least square (RLS) method. The method not only shows more stable performance in force tracking error, but also performs significantly better than traditional methods in complex environments, effectively solving the control stability and adaptability problems in different stiffness environments. Compared to other methods, the research contribution lies in improving the accuracy and reliability of the stripping action, providing new solutions for the automation and intelligence of power system maintenance.

## 3 Wire stripping motion of power distribution robot based on wire stripping and cutting force control algorithm and RLS

The research focuses on the optimization of PDR wire stripping motion, especially its application under the CGT mechanism. Firstly, a PDR wire stripper adapted to CGT is designed, followed by kinematic analysis based on WSCF control algorithm. Finally, an impedance control strategy based on RLS is introduced to address challenges in different stiffness environments and improve the stability and adaptability of the control system.

### 3.1 Design of wire stripper for power distribution robot under cylindrical gear transmission

CGT is widely used in the kinematic analysis of wire stripping in PDR, mainly due to its high efficiency and accuracy, stability and reliability, smooth motion characteristics, adaptability, and ease of maintenance. These characteristics make CGT very suitable for high-precision and strict WSO requirements, ensuring that robots can perform tasks stably and accurately in complex working environments (Mozaffari et al., 2020). CGT can provide high efficiency and precise transmission ratio, which is crucial for ensuring precise control of the wire stripper during the wire stripping process. The structure of cylindrical gears is relatively simple and stable, capable of withstanding large loads, which is crucial for maintaining stability and reliability during the wire stripping process. CGT can usually provide smooth motion, which helps reduce possible vibrations and impacts during the wire stripping process, thereby improving the quality of wire stripping. CGT can adapt to gears of different sizes and shapes, allowing it to be flexibly applied in different designs of wire strippers. This adaptability is crucial for the design of PDR as it needs to adapt to different working environments and task requirements.

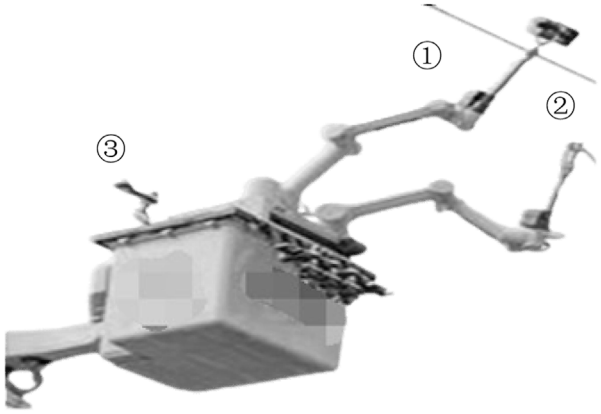


FIGURE 1
Schematic diagram of power distribution robot arm operation.

PDR is a comprehensive automated machine typically equipped with multiple robotic arms integrated on a mobile platform. Its main tasks include stripping of wire insulation layer, residual cleaning, application of conductive grease, installation of wire clamps, and design of end structures (Li N. et al., 2020). Meanwhile, robots need to be designed with insulation protection to ensure safe operation. Before manufacturing PDR, engineers will establish a virtual model for detailed simulation analysis and use it to construct the physical structure of the robot. Figure 1 is a schematic diagram of PDR tasks.

The control principle of the robotic arm can be seen in Figure 1, before WSD, the robot arm reduces wire swinging caused by wind or other interference by grasping and fixing wires. This process laid a stable foundation for subsequent operations. Afterwards, the robotic arm two will perform the stripping operation. The complex work environment and requirements for control stability may lead to incomplete wire stripping or damage to the metal core of the wire (Pei and Sun, 2023). After stripping the wire, the robotic arm uses cleaning tools to remove any residue from the exposed parts of the wire. Next, it will be exchanged for tools for applying conductive grease to improve the efficiency of electricity transmission. Afterwards, the robotic arm 3 will assist in installing the wire clamp to ensure the connection between the main high-voltage wire and the drainage wire. The entire process requires multiple robotic arms to work together, using master-slave control technology to ensure coordination and consistency. Figure 2 shows the PDR task structure.

From Figure 2, it can be seen that based on the control process of the robot arm in Figures 1, 2 further explores the operational structure of the robot. Especially in the scenario of how multiple robotic arms work together through master-slave control

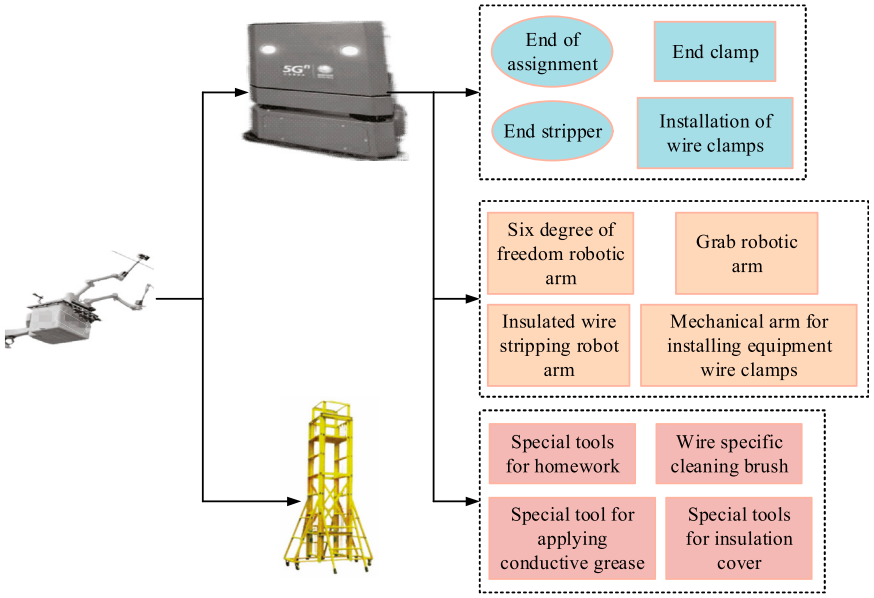


FIGURE 2
Operation structure of power distribution robot.

technology. The entire process requires the collaborative operation of multiple robotic arms to ensure task coordination and consistency. Specifically, Figure 2 shows robotic arms with different functions, including a Grab Robotic Arm for grasping, a Mechanical Arm for Stripping Robot for wire stripping, and a robotic arm for installing wire clamps. In addition, specialized tools and equipment were mentioned, such as cleaning brushes and special tools for applying conductive grease, which play an important role in preparing wire surfaces, ensuring good conductivity, and long-term performance. In the ever-changing environment of power distribution operations, the efficiency and quality of robots performing wire stripping tasks are significantly affected by the wire stripping technology they adopt. There are usually two main wire stripping technologies on the market, namely, straight cutting and rotary cutting. The direct cutting technique utilizes a pair of blades fixed inside the wire stripper to symmetrically cut the outer insulation along the wire in a 180° manner, and then rotate in the same direction once to loosen the layer. The rotary cutting stripping wire touches the wire at a certain angle through a single blade. The cutting tool in wire stripping moves slowly along the axial direction of the wire while rotating. But there are also challenges in controlling the stripping force, which usually rely on the operator's experience for adjustment.

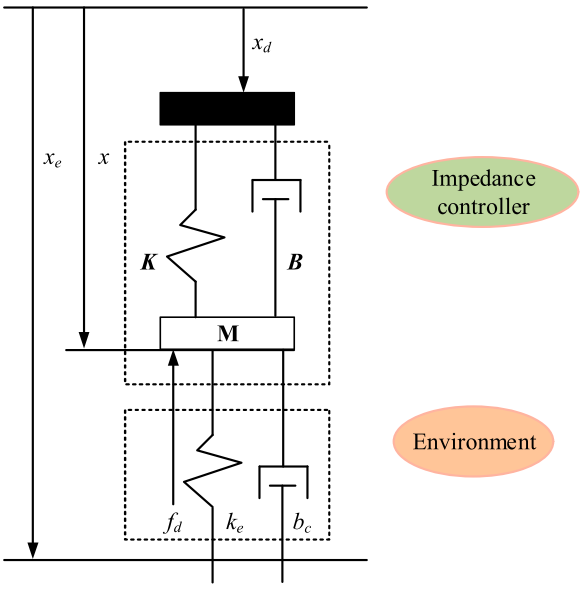


FIGURE 3
Impedance model of wire stripper in contact with wires.

## 3.2 Wire stripping motion of power distribution robot based on wire stripping and cutting force control algorithm

The WSO of PDR is a crucial link in the maintenance of distribution systems, which directly affects the efficiency and safety of the entire system. WSO requires high precision and stability, as inaccurate wire stripping may lead to wire damage or safety hazards. Traditional wire stripping techniques rely on the skills and experience of operators, which may lead to inconsistent and inefficient results in some cases. Therefore, developing an efficient, accurate, and automated wire stripping method has become crucial.

In power distribution operations, the end stripper used by robots faces many challenges when stripping the insulation layer of wires, such as the wire core being easily damaged or leaving insulation residue, which can affect the effectiveness of power distribution (Chen et al., 2023). To address these issues, the study employs the WSCF control algorithm for control. The interaction between the

end stripper of the robot and the wire is considered as a second-order dynamic system, and the dynamic principle is represented by Formula 1 (Li X. et al., 2020).

$$M_t\left(\ddot{X}-\ddot{X}_r\right)+B_t\left(\dot{X}-\dot{X}_r\right)+K_t\left(X-X_r\right)=F-F_r \tag{1}$$

In Formula 1, $M_t$, $B_t$, and $K_t$ are the inertia, damping, and stiffness matrices, which together determine the dynamic characteristics. $X_r$ and $X$ mean the parameter directions and actual directions of the end stripper, respectively. $\dot{X}_r$ and $X$ are the expected direction and actual direction, respectively. $\ddot{X}_r$ and $\ddot{X}$ refer to the expected and actual direction, respectively. $F_r$ and $F$ are the reference contact force and actual cutting force in the contact between the end stripper and the wire, respectively. Before the wire stripper comes into contact with the wire, the contact force remains zero, and a position tracking operation is performed at this time. As the wire stripper begins to come into contact with the wire, the impedance controller adjusts the position control command based on the deviation signal of the cutting force to correct the position deviation and combine it with the preset target position. In this process, the interaction between the wire stripper and the wire can be described by the impedance model in Figure 3, which covers the impedance characteristics of both the wire stripper end and the wire system.

In the cutting stage of the wire stripper, this action can be regarded as a one-dimensional scenario. In this case, force tracking and impedance control can be achieved through the method described in Formula 2 for design (Wang et al., 2022).

$$m_t\left(\ddot{x}-\ddot{x}_r\right)+b_t\left(\dot{x}-\dot{x}_r\right)+k_t\left(x-x_r\right)=f-f_r \tag{2}$$

In Equation 2, $m_t$ represents the quality of the system; $\ddot{x}$ is the actual location; $\ddot{x}_r$ is reference positions; $b_t$ representing the coefficient of friction; $\dot{x}$ and $\dot{x}_r$ represent the velocities of the actual position and the reference position respectively; $k_t$ indicate the elasticity coefficient of the spring; $f$ expressing external force; $f$ indicate reference force. After filtering the contact force deviation of the wire stripper, the correction amount of its position is obtained. Combined with the reference position value, the position control command is obtained, represented by Formula 3 (Choudhury et al., 2022).

$$x_d=x_r+x_f \tag{3}$$

In Equation 3, $x_d$ indicate the target location; $x_r$ indicate the reference position; $x_f$ indicate the location of the error. Finally, the position control command is converted into the driving voltage of the servo motor and implemented through the position controller. The servo motor responds to the driving voltage, precisely controls the PDR end effector, and implements meticulous wire stripping actions to ensure accurate execution and high-quality completion of the operation.

## 3.3 Impedance control based on RLS

To solve the inaccurate contact force caused by changes in environmental stiffness during wire stripping in PDR, an impedance force tracking control algorithm based on RLS is proposed. It can identify the insulation layer and core stiffness of the wire online, achieving precise force control of the wire stripper and smooth stripping of the wire. RLS is widely used in parameter identification due to its concise principle, efficient calculation, and ability to update parameters online. If the difference between the actual displacement and the assumed displacement is $\triangle x_e$, and the difference between the actual environmental stiffness and the assumed environmental stiffness is $\triangle k_e$, then Formula 4 can be obtained (Zhu et al., 2021).

$$\begin{cases}\triangle x_e=x_e-\widehat{x}_e\\ \triangle k_e=k_e-\widehat{k}_e\end{cases} \tag{4}$$

In Equation 4, $\triangle x_e$ represents the difference between the actual displacement and the assumed displacement; $x_e$ indicate actual displacement; $\widehat{x}_e$ indicating assumed displacement; $k_e$ and $\widehat{k}_e$ represent actual and assumed environments respectively. From this, Formula 5 can be obtained (Zhong et al., 2023a).

$$e_s=\frac{k_t}{k_e+k_t}\left(k_e\triangle x_e-\frac{\triangle k_e}{\widehat{k}_e}f_r\right) \tag{5}$$

In Equation 5, $e_s$ is the force deviation; $k_t$ is the damping coefficient; $k_t$ is the spring coefficient; $k_e\triangle x_e$ is the force deviation caused by the difference between the actual displacement and the assumed displacement; $-\frac{\triangle k_e}{\widehat{k}_e}f_r$ represents the force deviation caused by the difference between the actual environmental stiffness and the assumed environmental stiffness. In the operation of PDR, the main sources of force deviation are environmental stiffness and positional errors. Due to the usually small positional error in this situation, the deviation is mainly caused by environmental stiffness. The stiffness information of the wire is obtained by real-time updating of the reference position $x_r$ and utilizing online parameter identification technology based on RLS, achieving precise control of cutting force. In this framework, $\varphi(i)$ and $\phi(i)$ mean the ideal and actual output signals of the impedance force controller, respectively, so that the signal error can be calculated, represented by Formula 6 (Xiao et al., 2022).

$$e(i)=\phi(i)-\varphi(i) \tag{6}$$

In Equation 6, $e(i)$ represents signal error. By incorporating the forgetting factor $\lambda, \lambda\in(0,1]$, real-time monitoring of the dynamic changes in environmental stiffness can be achieved. Based on this, the corresponding iterative formula $L(n)$ is adjusted, and further power series expansion is performed on $L(n)$ to obtain Formula 7 (Brunke et al., 2022).

$$L(n)=e^2(n)+\lambda e^2(n-1)+\lambda^2e^2(n-2)+\cdots+\lambda^{n-1}e^2+\lambda^n e^2 \tag{7}$$

In Formula 7, $L(n)$ represents the sum of squared errors for the $n$ th iteration; $e^2(n)$ representing the square of the error for the $n$ th iteration; $\lambda$ represents the forgetting factor; $e^2(n-1)$ represents the square of the error for the $\lambda$ th iteration. In general, the coefficient of the squared series error is 1, indicating that if the forgetting factor is small, it is more inclined to balance the latest squared error, reducing the impact of earlier errors. In parameter identification, the identification effect is represented by error variance, and the mean error is used as the judgment threshold. When the error is less than the mean, it indicates that the system tends to stabilize. At this point, the forgetting factor $\lambda$ approaches 1, which helps to

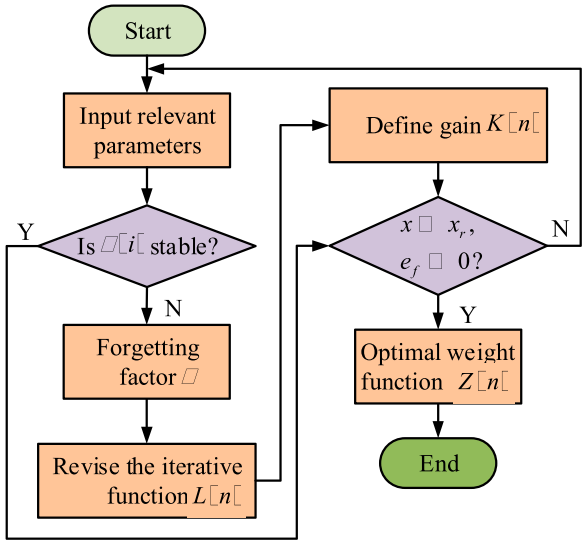


FIGURE 4
RLS algorithm process.

reduce identification errors. To improve the accuracy of stiffness parameter identification, theoretical analysis suggests that the optimal weight function must be determined. To achieve this goal, it is necessary to minimize the numerical value of the iterative function. By further simplifying this process, the final form of the weight function can be obtained, represented by Formula 8 (Ma et al., 2021).

$$Z(n) = Z(n-1) + K(n)e(n-1) \tag{8}$$

In Formula 8, $Z(n)$ is the weight function for the nth iteration; $Z(n-1)$ is the weight function of the $\lambda$ th iteration; $K(n)$ is the learning rate; $e(n-1)$ represents the error of the $\lambda$ th iteration. By using the above formula, the algorithm flow of RLS can be obtained in Figure 4.

Both environmental stiffness and positional errors can cause deviations in force control, therefore real-time updating of environmental stiffness and positional information is crucial for accurate force control. The calculation of cable stiffness is shown in Equation 9 (Mamakoukas et al., 2021).

$$EI = \sum_{i=1}^{n} E_i I_i \tag{9}$$

In Equation 9, $EI$ represents the total bending stiffness of the cable; $E_i$ indicate the elastic modulus of the $i$ layer material; $I_i$ representing the moment of inertia of the cross-section of the $i$ layer material; $n$ indicates the number of layers in the cable. When applying RLS for wire stripping in PDR, to reduce data errors, the study adopts the average value within the sampling period to represent the actual situation of the wire stripper's cutting force. When the error between this average value and the predetermined reference force is less than 0.001, it can be considered that the RLS impedance system is approaching stability, and the calculation of the least squares method can be stopped at this time. Finally, an algorithm is developed to update the identification of RLS stiffness parameters for the reference position of the cutting force, represented by Formula 10 (Kristiyono and Wiyono, 2021).

$$\begin{cases} x_r(t+1) = \dfrac{f_r}{k_e(t+1)} + x_e \\ x_d(t+1) = \dfrac{f_r}{k_e(t+1)} + x_e + x_f \end{cases} \tag{10}$$

In Equation 10, $x_r(t+1)$ indicate the position coordinates of the cutting force reference position at time $t+1$. $x_d(t+1)$ indicate the expected position at time $t+1$. $f_r$ is the force or applied force representing cutting force. $k_e(t+1)$ is the equivalent stiffness parameter of the system at time $t+1$. $x_e$ indicate the compensation position of the system. $x_f$ indicate additional compensation positions. In automation and intelligent control, parameter identification technology based on RLS is crucial for accurately modeling the dynamic characteristics of systems. In this study, the RLS parameter identification strategy is introduced to construct an impedance control model to optimize the performance of PDR wire stripping, ensuring high accuracy and stability under different working conditions. Figure 5 is an impedance control model based on RLS parameter identification.

Figure 5 shows the impedance control model based on RLS parameter identification, which includes seven parts: impedance controller, reference trajectory, trajectory correction mechanism, incremental position control, end stripper operation, RLS, and environmental stiffness perception. Specifically, the impedance controller is responsible for calculating the output signal based on the input signal. In this impedance control, the controller is designed based on the impedance characteristics of the simulated physical system, as shown in Equation 11.

$$F = MX_2 + BX_1 + KX_0 \tag{11}$$

In Equation 11, $F$ represents the applied force; $X_2$, $X_1$, $X_0$ represents the position, velocity, and acceleration of the object, respectively; $M$, $B$, $K$ represents the mass, damping, and stiffness of the object. The expected path provided by the reference trajectory to the control system serves as a reference; The trajectory correction part uses a PID controller to correct the deviation between the actual displacement and the reference displacement, ensuring that the system can move along the reference trajectory; The incremental position control part is a method of achieving the target position by continuously adjusting the position increment, used to adjust the control signal. The incremental position control equation is shown in Equation 12.

$$\Delta X = X_{\text{target}} - X_{\text{current}} \tag{12}$$

In Equation 12, $\Delta X$ represents the incremental position of the object; $X_{\text{target}}$ is the target location; $X_{\text{current}}$ is the current location. The end peeling operation is used to perform the actual peeling action, and the accuracy of peeling depends on the control model; The RLS part is used for online estimation of dynamic parameters such as wire stiffness, and the parameter evaluation formula is shown in Equation 13.

$$Y = \lambda\theta + \varepsilon \tag{13}$$

In Equation 13, $Y$ is the output of the system; $\lambda$ is the input vector; $\theta$ is the parameter vector to be estimated; $\varepsilon$ is noise. The environmental stiffness perception part is used to monitor and provide feedback on changes in environmental stiffness.

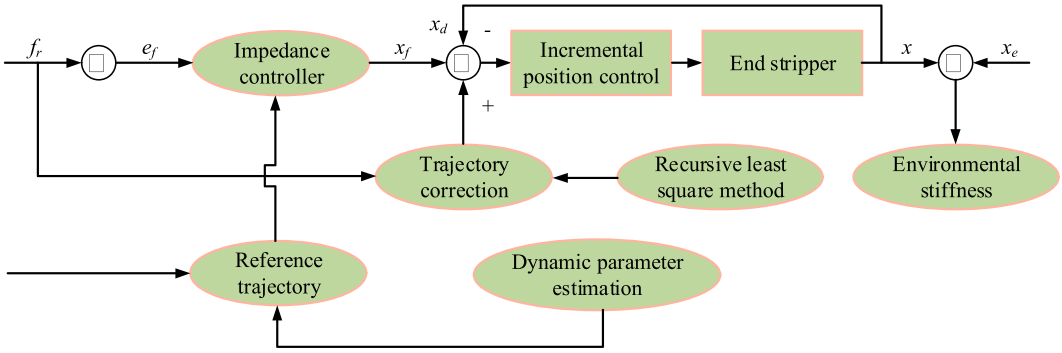


FIGURE 5
Impedance control model based on RLS parameter identification.

According to the derivation process of Equation 9, the control process of the control system is further analyzed from the perspective of practical application. Based on the derivation process of Equation 9, further analysis of the control process of the control system is conducted from the perspective of practical application. These together constitute a highly integrated and intelligent system aimed at achieving precise and stable wire stripping control.

## 4 Kinematic analysis of wire stripping for distribution robots based on wire stripping and cutting force control algorithm and RLS

A thorough analysis was conducted on the wire stripping motion of PDR under CGT. Through impedance control using WSCF control algorithm and RLS parameter identification, the effectiveness of these advanced technologies was first verified in a simulation environment. Then PDR wire stripping simulation analysis further confirmed the feasibility and efficiency of the entire system.

### 4.1 Impedance force control simulation analysis based on wire stripping and cutting force control algorithm and RLS parameter identification

After completing the necessary restrictions and startup instructions for the wire stripper, simulation experiments were conducted. The experiment used a cutting equipment model XYZ Precision Cutter Model XYZ1000 and a ForceSense FS-100 force sensor model for data acquisition. The environmental temperature control adopts THZ-300 constant temperature and humidity box. Collecting data specifically includes timestamp, cutting head position, cutting resistance, and environmental parameters. This experiment involved the contact and clamping of the wire stripper with the wire and the execution of the wire stripping task until it was completed. Then, the wire was released and restored to its initial position through a reverse rotating screw mechanism. The simulation duration of this process was a total of 13 s, with the wire stripping lasting for 4 s. This process could be modularized using Matlab/Simulink software. Figure 6 shows the sinusoidal force response and error curve based on the WSCF control algorithm and RLS parameter identification.

From Figure 6, it can be seen that under the control of the proposed method, the sinusoidal response force is smoother than without control. In Figure 6A, the proposed method shows that as the peeling time increases, the shear force varies within the range of [-8,18] without significant fluctuations. When there is no control force, the shear force curve fluctuates violently at 0.2 s, and the shear force fluctuates within the range of [-14, 20], which is 23% lower than the control force of the proposed method. This is due to the unevenness of the material and the fixed cutting parameters. As shown in Figure 6B, there is no significant difference in the error between the proposed method and the reference force ($P < 0.05$). The instability of shear force not only increases the risk of cutting errors, but may also cause damage to cutting equipment and the material being cut. Therefore, the results indicate that the dynamic adjustment mechanism of the proposed method ensures the stability and consistency of the cutting process. Afterwards, a comparison was performed on the constant force tracking response and error curve during stiffness sudden changes in Figure 7.

Figures 7A, B show the constant force response tracking curve and tracking error curve, respectively. In Figure 7A, the constant force response tracking curve of the research method shows relatively small fluctuations, and compared to the control force, the 3-s fluctuations are larger in the absence of control force. In addition, significant fluctuations in response force occur within the time range of (Amin et al., 2020; Zhang et al., 2023), which may be due to the control system automatically increasing cutting force to maintain cutting speed as material hardness increases. In Figure 7B, there is no significant difference in the error between the proposed method and the reference force ($P < 0.05$). The results indicate that this method has a good control effect on stiffness abrupt changes. To further explore its performance, the WSCF control algorithm with sudden stiffness changes and the sinusoidal force tracking and error curve for RLS parameter identification were analyzed in Figure 8.

Figures 8A, B show the sinusoidal force tracking response curve and the sinusoidal force tracking error, respectively. From Figure 8A, it can be seen that the shear force of the research method is greater

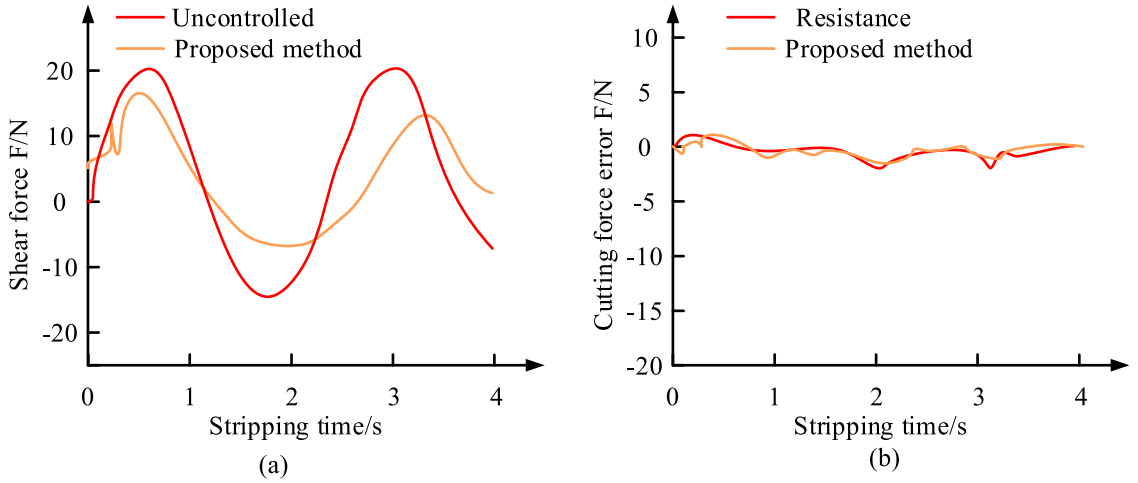


FIGURE 6
Comparison of cutting force changes between uncontrolled and controlled conditions. **(a)** Sinusoidal force response curves **(b)** Sine force tracking error curve.

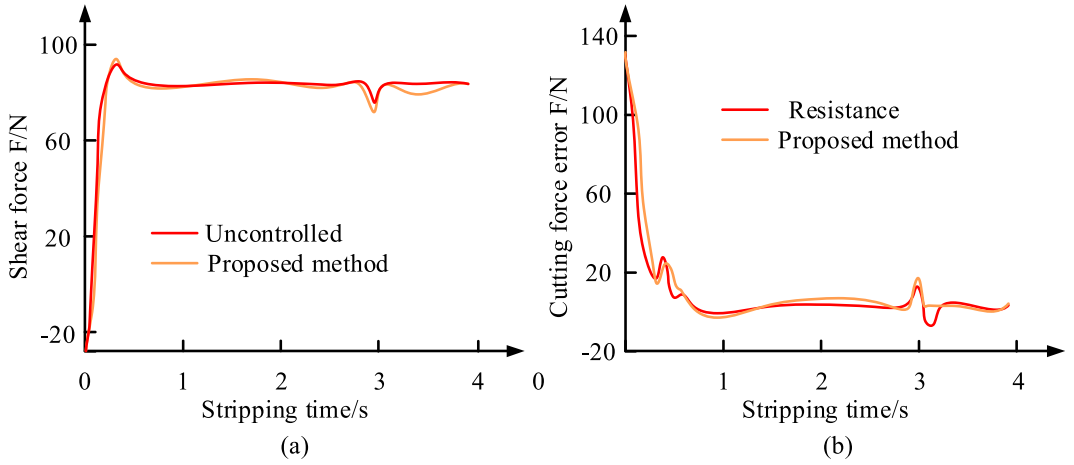


FIGURE 7
Tracking response and error curve with or without control force during sudden stiffness changes. **(a)** Constant force response tracking curve **(b)** Constant force tracking error curve.

than that without control, and the curve is more stable. At a peeling time of 1.9 s, the maximum impedance force of the proposed method reached −19.6 N, an increase of 66.3% compared to uncontrolled conditions. This may be due to the sudden change in stiffness caused by the increase in material hardness, thereby increasing the control force of the control system. In Figure 8B, the impedance force error curve of the research method has high stability, always around 0 N. There was no significant difference in the error between the proposed method and the reference force ($P < 0.05$). The results indicate that this method has good control accuracy and stability for sudden stiffness changes. The WSCF control algorithm with sudden stiffness changes and the slope force tracking and error curve for RLS parameter identification were analyzed in Figure 9.

Figures 9A, B show the slope force tracking response curve and slope force tracking error, respectively. In Figure 9A, The impedance force of the research method almost matched the reference force, while the general impedance force had a significant difference from the reference force. After 2 s of wire stripping, the impedance force of the research method and the reference force were both 81.3 N, and the general impedance force had not stabilized until it stabilized at 3.0s, with an impedance force of 78.1 N. This indicates that the research method has better control effect than general impedance force, and can quickly respond and adjust resistance. In Figure 9B, the impedance force error curve of the research method tended to stabilize after 2 s, approaching 0N, while the general impedance force error curve had significant fluctuations. There was no significant difference in the error between the proposed method and the reference force ($P < 0.05$). This indicates that the research method can not only effectively control resistance, but also quickly stabilize the cutting process, reducing unnecessary fluctuations and errors.

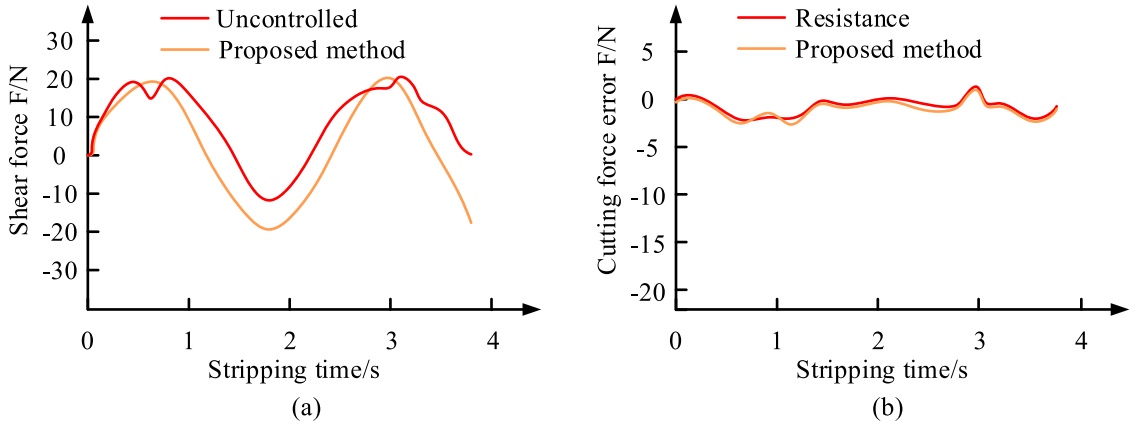


FIGURE 8
Comparison of sinusoidal force tracking and error curves with and without control. **(a)** Sinusoidal force tracking error **(b)** Sinusoidal force tracking response curve.

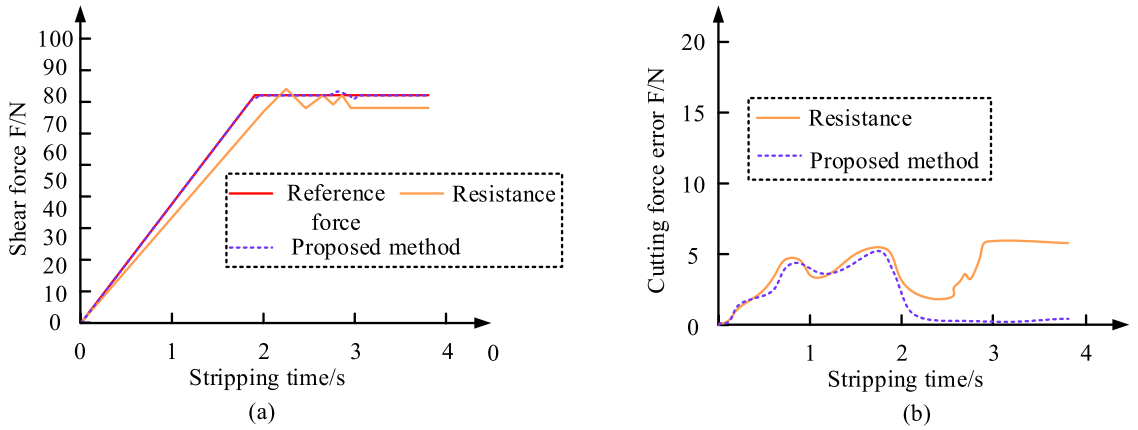


FIGURE 9
Slope force tracking and error curve of the proposed method. **(a)** Slope force tracking response curve **(b)** Slope force tracking error.

## 4.2 Simulation analysis of wire stripping for power distribution robots

As automation and intelligence improve, PDR plays an increasingly important role in power system maintenance. Especially in the critical operation of wire stripping, efficient and accurate automation not only improves operational efficiency but also reduces the need for manual intervention. Through simulation research, new control algorithms and technologies such as WSCF control algorithm and RLS can be verified for their application in impedance control. This is very important for promoting technological innovation and improving practical applications. Table 1 shows the experimental parameters of PDR.

When conducting wire stripping experiments, the wire stripper itself remains stable without component deformation or unstable shaking. During the WSO process, there was no damage or insulation residue on the surface of the wire, and the wire stripping control error remained within an acceptable range. These indicate that the structure of the wire stripper and the wire stripping control algorithm are both effective. Figure 10 shows the experimental and simulation data of PDR.

Figures 10A, B show the experimental and simulation data of PDR, respectively. The impedance force of the research method almost matched the reference force, while the general impedance force had a significant difference from the reference force. After 2 s of wire stripping, the impedance force of the research method and the reference force were both 81.3N, and the general impedance force had not stabilized until it stabilized at 3.0s, with an impedance force of 78.1 N. Meanwhile, the impedance force error curve of the research method tended to stabilize after 2 s, approaching 0N, while the general impedance force error curve had significant fluctuations. Figure 11 shows the results of the wire stripping test.

Figures 11A, B show the stripping test results of the impedance control method based on WSCF control algorithm and RLS, as well as the general wire stripping method, respectively. Under the WSCF control algorithm and RLS impedance control, the wire stripping surface was smooth and undamaged, demonstrating the rationality of wire stripper design and the superiority of wire stripping control

TABLE 1 Experimental parameter settings for power distribution robots.

| Number | Project | Content | Unit |
|---|---|---|---|
| (1) | Distribution network | 10 | kv |
| (2) | Steel core aluminum stranded wire | Nominal cross-section aluminum/steel 150/20 | — |
| (3) | Steel ratio | 13 | % |
| (4) | Insulation thickness | 3.3 | mm |
| (5) | Number of single wires: aluminum | 24 | root |
| (6) | Number of single wires: steel | 7 | root |
| (7) | Steel core diameter | 5.56 | mm |
| (8) | Line diameter | 16.6 | mm |

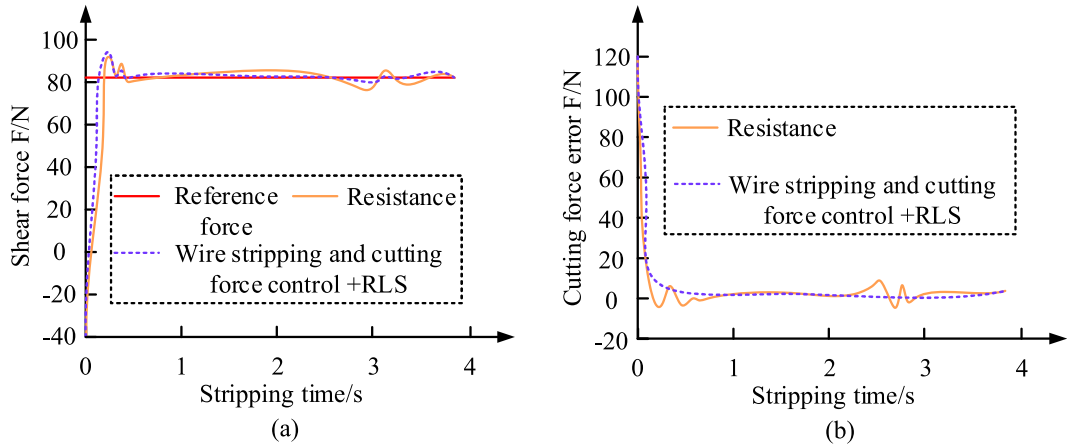


FIGURE 10
Comparison results between experimental data and simulation data. **(a)** Test data **(b)** SImulation data.

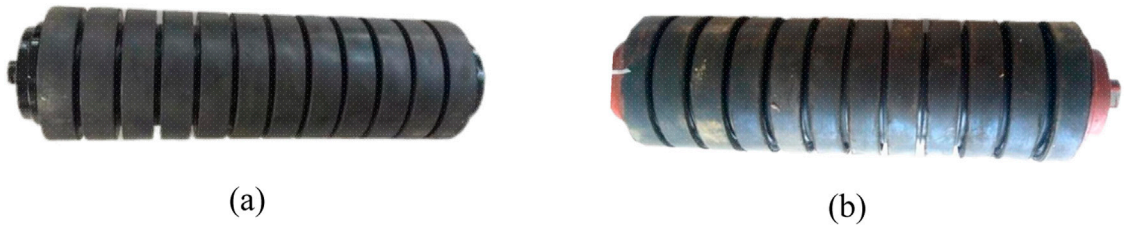


FIGURE 11
Stripping test results. **(a)** Wire stripping and cutting force control +RLS. **(b)** General wire stripping.

algorithm. Although general impedance control experiments could also complete wire stripping tasks, the results were not ideal and had not met the high standards required for power distribution operations. To further validate the effectiveness of the proposed method in performing wire stripping tasks, precision, operational efficiency, and stability were used as evaluation indicators for robot control. And combined with 5 classic robot control methods: PID based Wire Stripping Motion Analysis (PID-WSMA), Fuzzy Logic based Wire Stripping Motion Analysis (F-WSMA), Neural Network based Wire Stripping Motion Control (NN-WSMA), B-spline Wavelet Neural Network based Wire Stripping Motion Control (BWNN-WSMA), and Logarithmic Sliding Mode based Wire Stripping Motion Control (LSM-WSMA), the results are shown in Table 2.

Table 2 compares the performance of multiple wire stripping methods on three key indicators: wire stripping accuracy, wire stripping efficiency, and system stability. The proposed method is significantly superior to other methods in all aspects, with an accuracy of 98.5%, an efficiency of 1.6 m/min, and a system stability

TABLE 2 Comparison of control performance of various methods and measurement methods.

| Method | Wire stripping accuracy (%) | Stripping efficiency (m/min) | System stability (rating, 1–10) |
|---|---|---|---|
| Proposed | 98.5 | 1.6 | 9.5 |
| PID-WSMA (Deng et al., 2019) | 91.2 | 1.0 | 8.2 |
| F-WSMA (Zhong et al., 2023b) | 93.2 | 1.1 | 8.1 |
| NN-WSMA (Li et al., 2021) | 91.9 | 1.2 | 8.8 |
| BWNN-WSMA (Liu et al., 2023) | 92.1 | 0.9 | 8.2 |
| LSM-WSMA (Dong et al., 2022) | 91.9 | 1.0 | 8.1 |
| Calculation method | Accuracy = (Number of successful wire-stripping operations/Total wire-stripping attempts) × 100% | Stripping efficiency = Length of wire stripped/Operation time | Evaluated by experts |

score of 9.5, demonstrating comprehensive performance advantages. In contrast, the accuracy of other methods generally ranges from 91.2% to 93.2%, the efficiency is between 0.9 and 1.2 m/min, and the stability score is between 8.1–8.8, showing similar performance but significantly lower than the proposed method. Among them NN-WSMA performs slightly better than other comparative methods in accuracy (91.9%) and efficiency (1.2 m/min), while BWNN-WSMA performs the worst in efficiency (0.9 m/min). Overall, the proposed method has significant comprehensive performance advantages in wire stripping tasks and is currently the optimal solution.

## 5 Conclusion

The stripping task of PDR in carrying out power line maintenance operations is a key link in ensuring the stable operation of the power grid, requiring precise stripping actions to prevent damage to the wires and ensure connection quality. This study combined the advantages of compact structure, high transmission efficiency, and strong adaptability of CGT to construct a PDR wire stripper design. Then the WSCF control algorithm was applied to the PDR wire stripping motion, and impedance control based on RLS was added. In the simulation results, whether in constant force tracking, sine force tracking, or slope force tracking, the impedance control strategy based on WSCF control algorithm and RLS parameter identification exhibited rapid and stable adaptability when the environmental stiffness encountered sudden changes. And its error continued to approach zero. After 2 s of wire stripping, the impedance force of the research method and the reference force were both 81.3 N, and the general impedance force had not stabilized until it stabilized at 3.0 s, with an impedance force of 78.1 N. The impedance force error curve of the proposed method shows no significant difference compared to the general impedance force error curve ($P < 0.05$). The efficiency and accuracy of this response demonstrate the effectiveness of WSCF control algorithm, RLS parameter identification technology, and impedance control algorithm. The control performance of the proposed method is superior to the three classic algorithms PID-WSMA, F-WSMA, and NN-WSMA, with an average score of 1.5%, 0.27 m/min, and 0.8 points higher in accuracy, efficiency, and stability, respectively. There are still some shortcomings in this study, such as the experiment only targeting a specific type of high-voltage wire. Different types of high-voltage conductors have their own insulation layer thickness and core characteristics, which increases the complexity of the operating environment and may introduce additional uncertainty factors into the control system. Although current control algorithms have shown effectiveness for specific wire types, to achieve widespread applicability, it is necessary to conduct scalability testing and experimental verification on multiple wire types. Due to the limitations of experimental conditions, discussing label noise and data dispersion can be considered as a future research direction to increase the generalization ability of the method.

## Data availability statement

The original contributions presented in the study are included in the article/supplementary material, further inquiries can be directed to the corresponding author.

## Author contributions

JL: Data curation, Formal Analysis, Investigation, Writing–original draft, Writing–review and editing. ZQ: Conceptualization, Methodology, Writing–original draft, Writing–review and editing.

## Funding

The author(s) declare that no financial support was received for the research, authorship, and/or publication of this article.

## Conflict of interest

The authors declare that the research was conducted in the absence of any commercial or financial relationships that could be construed as a potential conflict of interest.

## Publisher's note



## References

Amin, F., Sulaiman, E., Utomo, W. M., Khan, F., and Omar, M. F. (2020). Development of single phase 12S-6P FEFSM and field oriented control algorithm based on the effect of rotor position on stator flux pair linkage. *IET Electr. Power Appl.* 14 (8), 1458–1468. doi:10.1049/iet-epa.2019.0607

Arastou, A., Rabieyan, H., and Karrari, M. (2022). Inclusive modelling and parameter estimation of a steam power plant using an LMI-based unknown input reconstruction algorithm. *IET generation, Transm. and distribution* 16 (7), 1425–1437. doi:10.1049/gtd2.12379

Bieze, T. M., Kruszewski, A., Carrez, B., and Duriez, C. (2020). Design, implementation, and control of a deformable manipulator robot based on a compliant spine. *Int. J. Robotics Res.* 39 (14), 1604–1619. doi:10.1177/0278364920910487

Brahmi, B., Saad, M., Rahman, M. H., and Brahmi, A. (2020). Adaptive force and position control based on quasi-time delay estimation of exoskeleton robot for rehabilitation. *IEEE Trans. Control Syst. Technol.* 28 (6), 2152–2163. doi:10.1109/tcst.2019.2931522

Brunke, L., Greeff, M., Hall, A. W., Yuan, Z., Zhou, S., Panerati, J., et al. (2022). Safe learning in robotics: from learning-based control to safe reinforcement learning. *Annu. Rev. Control, Robotics, Aut. Syst.* 5 (1), 411–444. doi:10.1146/annurev-control-042920-020211

Chen, Y., Wang, Y., Tang, X., Wu, K., Wu, S., Guo, R., et al. (2023). Intelligent power distribution live-line operation robot systems based on stereo camera. *High. Volt.* 8 (6), 1306–1318. doi:10.1049/hve2.12349

Choudhury, S., Gupta, J. K., Kochenderfer, M. J., Sadigh, D., and Bohg, J. (2022). Dynamic multi-robot task allocation under uncertainty and temporal constraints. *Aut. Robots* 46 (1), 231–247. doi:10.1007/s10514-021-10022-9

Deng, Y., Wu, C., Zhang, X., and Jia, X. (2019). Examining the effectiveness of weighted spectral mixture analysis (WSMA) in urban environments. *Int. J. Remote Sens.* 40 (8), 3055–3075. doi:10.1080/01431161.2018.1539270

Dong, H., Yang, X., and Basin, M. V. (2022). Practical tracking of permanent magnet linear motor via logarithmic sliding mode control. *IEEE/ASME Trans. Mechatronics* 27 (5), 4112–4121. doi:10.1109/tmech.2022.3142175

Jiang, Y., Meng, H., Chen, G., Yang, C., Xu, X., Zhang, L., et al. (2022). Differential-steering based path tracking control and energy-saving torque distribution strategy of 6WID unmanned ground vehicle. *Energy* 254 (Sep.1 Pt.A), 124209–124215. doi:10.1016/j.energy.2022.124209

Kristiyono, R., and Wiyono, W. (2021). Autotuning fuzzy PID controller for speed control of BLDC motor. *J. Robotics Control (JRC)* 2 (5), 400–407. doi:10.18196/jrc.25114

Li, H., Ji, S., Jiang, Y., and Chu, J. (2021). Parameter study and experimental analysis of a scraping de-icing concept for thin ice using end-of-life wire ropes. *J. Mech. Sci. Technol.* 35 (8), 3395–3406. doi:10.1007/s12206-021-0713-y

Li, L., and Gao, Z. (2020). Maximization of wave power extraction of a heave point absorber with a sea-state-based causal control algorithm. *Energy* 204 (Aug.1), 117881. doi:10.1016/j.energy.2020.117881

Li, N., Zhai, Y., Jiang, J., and Wei, D. (2020a). Micro-control technology of biomedical robot based on optimized recognition algorithm. *Basic and Clin. Pharmacol. and Toxicol.* 127 (S2), 6.

Li, X., Korad, A. S., and Balasubramanian, P. (2020b). Sensitivity factors based transmission network topology control for violation relief. *IET Generation Transm. and Distribution* 14 (17), 3539–3547. doi:10.1049/iet-gtd.2019.1196

Liu, Z., Gao, H., Yu, X., Lin, W., Qiu, J., Rodríguez-Andina, J. J., et al. (2023). B-spline wavelet neural-network-based adaptive control for linear-motor-driven systems via a novel gradient descent algorithm. *IEEE Trans. Industrial Electron.* 71 (2), 1896–1905. doi:10.1109/tie.2023.3260318

Ma, H., Zhou, Q., Li, H., and Lu, R. (2021). Adaptive prescribed performance control of a flexible-joint robotic manipulator with dynamic uncertainties. *IEEE Trans. Cybern.* 52 (12), 12905–12915. doi:10.1109/tcyb.2021.3091531

Mamakoukas, G., Castano, M. L., Tan, X., and Murphey, T. D. (2021). Derivative-based Koopman operators for real-time control of robotic systems. *IEEE Trans. Robotics* 37 (6), 2173–2192. doi:10.1109/tro.2021.3076581

Mozaffari, S., Akbarzadeh, M., and Vogel, T. (2020). Graphic statics in a continuum: strut-and-tie models for reinforced concrete. *Comput. and Struct.* 240 (Nov), 106335–106335.16. doi:10.1016/j.compstruc.2020.106335

Pei, S., and Sun, H. (2023). Structural design and simulation study of intelligent defect elimination equipment for high-voltage transmission line pin defects. *IET Generation, Transm. and Distribution* 17 (24), 5366–5377. doi:10.1049/gtd2.13049

Roberts, J., and Florentine, S. (2021). Biology, distribution and control of the invasive species Ulex europaeus (Gorse): a global synthesis of current and future management challenges and research gaps. *Weed Res.* 61 (4), 272–281. doi:10.1111/wre.12491

Stefenon, S. F., Seman, L. O., Pavan, B. A., Ovejero, R. G., and Leithardt, V. R. Q. (2022). Optimal design of electrical power distribution grid spacers using finite element method. *IET generation, Transm. and distribution* 16 (9), 1865–1876. doi:10.1049/gtd2.12425

Wang, C., Gao, Q., Gao, W., and Ouyang, J. (2022). Discussion about calculation method of light transmission efficiencies of elbows in cylindrical light pipes. *Sol. Energy* 238 (May), 39–43. doi:10.1016/j.solener.2022.04.024

Xiao, X., Liu, B., Warnell, G., and Stone, P. (2022). Motion planning and control for mobile robot navigation using machine learning: a survey. *Aut. Robots* 46 (5), 569–597. doi:10.1007/s10514-022-10039-8

Xu, S., Wu, J., Zhang, S., and Yang, X. (2022). Hydrodynamic analysis of a tethered underwater robot with control equipment subjected to cnoidal waves. *Ocean. Eng.* 243 (Jan.1), 110264–110264.17. doi:10.1016/j.oceaneng.2021.110264

Zhang, G., Wang, L. X., Li, J., and Zhang, W. (2023). Improved LVS guidance and path-following control for unmanned sailboat robot with the minimum triggered setting. *Ocean. Eng.* 272 (Mar.15), 113860–113861.9. doi:10.1016/j.oceaneng.2023.113860

Zhao, W., Han, F., Qiu, X., Peng, X., Zhao, Y., and Zhang, J. (2023). Research on the identification and distribution of biofouling using underwater cleaning robot based on deep learning. *Ocean. Eng.* 273 (Apr.1), 113909. doi:10.1016/j.oceaneng.2023.113909

Zhong, J., Wang, Z., Hu, S., and Han, Z. (2023b). A novel 10 kV high-voltage cable stripping robot's mechanism design and analysis. *Robotica* 41 (9), 2605–2624. doi:10.1017/s0263574723000565

Zhong, J., Wang, Z., Hu, S., Hu, S., and Han, Z. (2023a). A novel 10 kV high-voltage cable stripping robot's mechanism design and analysis. *Robotica* 41 (9), 2605–2624. doi:10.1017/s0263574723000565

Zhu, W., Guo, X., Owaki, D., Kutsuzawa, K., and Hayashibe, M. (2021). A survey of sim-to-real transfer techniques applied to reinforcement learning for bioinspired robots. *IEEE Trans. Neural Netw. Learn. Syst.* 34 (7), 3444–3459. doi:10.1109/tnnls.2021.3112718